

Green Fluorescent Protein as a Noninvasive Intracellular pH Indicator

Malea Kneen, Javier Farinas, Yuxin Li, and A. S. Verkman

Departments of Medicine and Physiology, Cardiovascular Research Institute, University of California, San Francisco, California 94143 USA

ABSTRACT It was found that the absorbance and fluorescence of green fluorescent protein (GFP) mutants are strongly pH dependent in aqueous solutions and intracellular compartments in living cells. pH titrations of purified recombinant GFP mutants indicated >10-fold reversible changes in absorbance and fluorescence with pK_a values of 6.0 (GFP-F64L/S65T), 5.9 (S65T), 6.1 (Y66H), and 4.8 (T203I) with apparent Hill coefficients of 0.7 for Y66H and ~ 1 for the other proteins. For GFP-S65T in aqueous solution in the pH range 5–8, the fluorescence spectral shape, lifetime (2.8 ns), and circular dichroic spectra were pH independent, and fluorescence responded reversibly to a pH change in <1 ms. At lower pH, the fluorescence response was slowed and not completely reversed. These findings suggest that GFP pH sensitivity involves simple protonation events at a pH of >5, but both protonation and conformational changes at lower pH. To evaluate GFP as an intracellular pH indicator, CHO and LLC-PK1 cells were transfected with cDNAs that targeted GFP-F64L/S65T to cytoplasm, mitochondria, Golgi, and endoplasmic reticulum. Calibration procedures were developed to determine the pH dependence of intracellular GFP fluorescence utilizing ionophore combinations (nigericin and CCCP) or digitonin. The pH sensitivity of GFP-F64L/S65T in cytoplasm and organelles was similar to that of purified GFP-F64L/S65T in saline. NH_4Cl pulse experiments indicated that intracellular GFP fluorescence responds very rapidly to a pH change. Applications of intracellular GFP were demonstrated, including cytoplasmic and organellar pH measurement, pH regulation, and response of mitochondrial pH to protonophores. The results establish the application of GFP as a targetable, noninvasive indicator of intracellular pH.

INTRODUCTION

The green fluorescent protein (GFP) from the jellyfish *Aequorea victoria* is used widely as a noninvasive fluorescent marker for gene expression, protein localization, and intracellular protein targeting (Gerdes and Kaether, 1996; Chalfie et al., 1994; Cubitt et al., 1995). Structural analysis by x-ray crystallography indicated that the GFP protein consists of a β -barrel in which the oxidized triamino acid chromophore is buried in the protein interior (Yang et al., 1996; Örmö et al., 1996). Various GFP mutants have been generated that have altered physico-chemical properties, including fluorescence excitation and emission maxima, molar absorbance, and chromophore oxidation kinetics (Heim et al., 1994, 1995; Andersen et al., 1996; Cormack et al., 1996; Kimata et al., 1997). GFP has been expressed in bacteria, plants, yeast, mammalian cells, and whole organisms (Lim et al., 1995; Zolotukhin et al., 1996; Hampton et al., 1996). GFP has also been expressed in subcellular organelles by fusion with appropriate targeting sequences (Rizzuto et al., 1995, 1996; DeGiorgi et al., 1996; Girotti and Banting, 1996; Terasaki et al., 1996; Hampton et al., 1996; Cole et al., 1996; Liu et al., 1997).

GFP and selected mutants have considerable potential as noninvasive sensors of biologically important intracellular functions. Our lab used GFP as a reporter molecule to probe

the microviscosity of cytoplasm (Swaminathan et al., 1997) and mitochondria (Partikian et al., 1998) by fluorescence photobleaching and time-resolved fluorescence methods. Energy transfer between GFP mutants was exploited in the design of a protease sensor in which blue and green fluorescent GFP mutants were linked by a spacer containing a trypsin cleavage site (Heim and Tsien, 1996). A GFP-based fluorescence sensor of calcium was developed recently based on energy transfer between blue and green fluorescent GFP mutants linked by a calmodulin-binding sequence (Romoser et al., 1997; Miyawaki et al., 1997).

The purpose of this study was to evaluate the suitability of GFP as an intracellular pH indicator. Although early studies on native GFP noted the pH sensitivity of absorbance and fluorescence (Bokman and Ward, 1981; Ward et al., 1980, 1982), the mechanism of GFP pH sensitivity has not been investigated, nor has the possibility been explored that GFP might be used as a pH sensor in living cells. We found that the fluorescence of GFP is very sensitive to pH in vitro and in vivo, and that its pH sensitivity could be modified by point mutations. GFP fluorescence responded rapidly and reversibly to pH changes. Cell experiments indicated that GFP is suitable as a noninvasive pH indicator for study of pH regulation in intracellular compartments that cannot be labeled with conventional pH indicators.

MATERIALS AND METHODS

Cell culture

CHO-K1 cells (ATCC CRL9618) and LLC-PK1 cells (CL101.1) were cultured on 18-mm-diameter round glass coverslips at 37°C in 95% air, 5% CO_2 . CHO cells were cultured in Ham's F12 medium, and LLC-PK1 cells in DME-H21, each containing 10% fetal bovine serum, penicillin (100

Received for publication 25 September 1997 and in final form 3 December 1997.

Address reprint requests to Dr. Alan S. Verkman, Cardiovascular Research Institute, 1246 Health Sciences East Tower, Box 0521, University of California, San Francisco, San Francisco, CA 94143-0521. Tel.: 415-476-8530; Fax: 415-665-3847; E-mail: verkman@itsa.ucsf.edu.

© 1998 by the Biophysical Society

0006-3495/98/03/1591/09 \$2.00

U/ml) and streptomycin (100 $\mu\text{g/ml}$). Cells were transfected 1 day after plating (at $\sim 80\%$ confluence) with 1 μg of plasmid DNA encoding the various GFP fusion proteins and 12 μg of Lipofect-AMINE reagent (BRL, Bethesda, MD) in a 0.2-ml volume of OPTI-MEM (BRL). The transfection mixture was replaced with 1 ml of culture medium at 5 h. Cells were used 2–3 days after transfection.

Plasmid constructions

The coding sequence of GFP-F64L/S65T was PCR amplified from plasmid pEGFP-C1 (Clontech) using primers: sense, 5'-GGAATTCGTGAGCAAGGGCGAGGAGCTGTTCAC-3'; antisense, 5'-GCTCTAGATTACTTGTACAGCTCGTCCATGCCG-3' (engineered *EcoRI* and *XbaI* sites underlined). The targeting construct for GFP-F64L/S65T expression in cytoplasm was prepared as described in Swaminathan et al. (1997) except for replacement of GFP-S65T by GFP-F64L/S65T. For mitochondrial targeting, the targeting presequence of subunit VIII of human cytochrome c oxidase (COX) (Rizzuto et al., 1995) was polymerase chain reaction (PCR) amplified using human kidney cDNA as template and the following primers: sense, 5'-GCCCCAAGCTTATCATGTCCGTCCTGACGCC-3'; antisense, 5'-CGGAATTCCTTCCCCTCCGGCGGC-AACG-3' (engineered *HindIII* and *EcoRI* restriction sites underlined). The COX8 targeting sequence was subcloned into eukaryotic expression vector pcDNA3.1 (Invitrogen Corp., San Diego, CA) at *HindIII/EcoRI* sites and ligated upstream and in frame with GFP-F64L/S65T at *EcoRI/XbaI* sites. For Golgi targeting, a cDNA fragment encoding residues -77 to -31 of the human β -1,4-galactosyltransferase (Masri et al., 1988) signal peptide was PCR amplified using human kidney cDNA as template and the following primers: sense, 5'-GCCCCAAGCTTAAGATGAGGCTTCGGAGCC-3'; antisense, 5'-CGGAATTCGCTCAGGTCCGGCC-CAGCCA-3' (engineered *HindIII* and *EcoRI* restriction sites underlined). The fragment was subcloned into pcDNA3.1 at *HindIII/EcoRI* sites, and the GFP fragment was ligated downstream and in frame at *EcoRI/XbaI* sites. For endoplasmic targeting, a cDNA fragment encoding residues -30 to 8 of bovine preprolactin (Sasavage et al., 1982) was amplified using plasmid pSP-BPI as template and the following primers: sense, 5'-GCCCCAAGCTTACCATGGACAGCAAAGGTTTC-3'; antisense, 5'-CGGAATTCAGGCCCATTTGGGACAGACGG-3' (engineered *HindIII* and *EcoRI* sites underlined), and subcloned into pcDNA3.1 at *HindIII/EcoRI* sites. The GFP coding sequence was subcloned downstream and in frame as above, except that a SEKDEL sequence (Munro and Pelham, 1987) was introduced at the GFP carboxy terminus by PCR amplification using antisense primer 5'-GCTCTAGACTACAACCTCATCTTTTCTGAC TTGTACAGCTCGTCCATGCG-3', where an engineered *ApaI* site is underlined and the sequence encoding SEKDEL is in bold. Constructs were confirmed by sequence analysis.

GFP expression and purification

GFPs S65T, T203I, Y66H, and F64L/S65T were purified by Ni-affinity chromatography after subcloning into plasmid pRSET, expression in *Escherichia coli* BL21(DE3), and bacterial lysis as described in Swaminathan et al. (1997). Proteins eluted from the affinity column were judged to be $>98\%$ pure by Coomassie-stained sodium dodecyl sulfate polyacrylamide gel electrophoresis. Proteins were dialyzed against 5 mM sodium phosphate (pH 7.4) and lyophilized.

Spectroscopic measurements

Fluorescence spectra were recorded on an SLM 8000c fluorimeter (SLM Instruments, Urbana, IL). The fluorescence signal was normalized to a quantum counter in the reference channel. Excitation and emission monochromator slit widths were 4 nm. Fluorescence was corrected for background, dilution, and the inner filter effect as needed (generally, $<3\%$ correction). All measurements were performed at room temperature. Fluorescence lifetimes were measured on an SLM 48000 MHF fluorimeter by

multi-frequency phase-modulation fluorimetry. Excitation wavelength was 488 nm with fluorescein in 0.1 N NaOH (lifetime, 4.0 ns) as lifetime reference. Stopped-flow fluorescence measurements were done on a Hi-Tech SF51 instrument at 480 nm excitation and >515 nm emission wavelengths. A suspension of GFP-S65T in buffer A at specified initial pH was mixed with an equal volume of buffer A titrated to give a specified final pH after mixing. The instrument mixing and dead times were less than 1.5 ms. Absorbance spectra were measured on an HP8452 photodiode array spectrophotometer (Hewlett-Packard). CD spectra were acquired over 200–260 nm on a Jasco J-500A spectropolarimeter using a 0.5-mm-pathlength quartz cell.

pH titration and quenching experiments

Titration of GFP fluorescence versus pH were performed by cuvette fluorimetry. Purified GFPs (3–10 $\mu\text{g/ml}$) were dissolved in buffer A containing (in mM): 120 KCl, 5 NaCl, 0.5 CaCl₂, 0.5 MgSO₄, 10 MES, 10 MOPS, 10 citrate, pH 8.00. Predetermined aliquots of 1 N HCl were slowly added with rapid stirring to titrate pH from 8.00 to 4.00 by 0.50 pH unit intervals. Fluorescence quenching titrations with acrylamide were performed using a 5 M acrylamide stock solution.

Fluorescence microscopy

Cell fluorescence was measured using an inverted epifluorescence microscope (Nikon Diaphot). Coverglasses containing cultured cells were mounted in a laminar-flow perfusion chamber and viewed with an oil immersion objective (Nikon Plan-Apo 40 \times , N.A. 1.3). Cells were illuminated by a 100-W tungsten/halogen lamp powered by a stabilized direct current power supply (Oriel). A neutral density filter was used to attenuate the excitation light intensity, and an adjustable field diaphragm reduced illuminated field to a small group of cells (generally 10–20). Wavelength selection was accomplished using an HQ GFP filter set (excitation, 480 \pm 20 nm; dichroic, 495 nm; emission, 510 \pm 20 nm; Chroma Corp., Brattleboro, NJ). Emitted fluorescence was detected using a photomultiplier, amplifier, and analog-to-digital converter. Imaging was done on a Leitz epifluorescence microscope equipped with a Nipkow wheel coaxial confocal attachment (Technical Instruments, San Francisco, CA). Cells were viewed with a 60 \times oil immersion objective (Nikon Plan-Apo, N.A. 1.4) for detection of confocal fluorescence images by a cooled CCD camera.

In vivo pH calibration

Coverslips containing GFP-F64L/S65T-transfected cells were mounted in the perfusion chamber and perfused initially for 1–5 min with PBS (in mM): 137 NaCl, 2.7 KCl, 0.7 CaCl₂, 1.1 MgCl₂, 1.5 KH₂PO₄, 8.1 Na₂HPO₄, pH 7.4, at 2–10 ml/min. The perfusate was then switched to a series of calibration solutions (buffer B) containing (in mM) 120 KCl, 20 NaCl, 0.5 CaCl₂, 0.5 MgSO₄, and 20 HEPES and 5–10 μM nigericin and 10–20 μM CCCP, pH 4.00–8.00 (in 0.5 pH unit intervals). In some experiments the ionophores were replaced by digitonin (0.005% w/v).

RESULTS

It was found that the fluorescence and absorbance properties of various GFP mutant proteins were strongly pH dependent. Fig. 1 A shows fluorescence excitation and emission spectra of GFP-S65T. Although the shape of the spectra did not change significantly with pH, the intensities decreased progressively with lowered pH, decreasing to 50% of maximal intensity at a pH of ~ 6.0 . An absorbance titration was done to determine whether the molar extinction of GFP-S65T was pH dependent (Fig. 1 B). Two absorbance max-

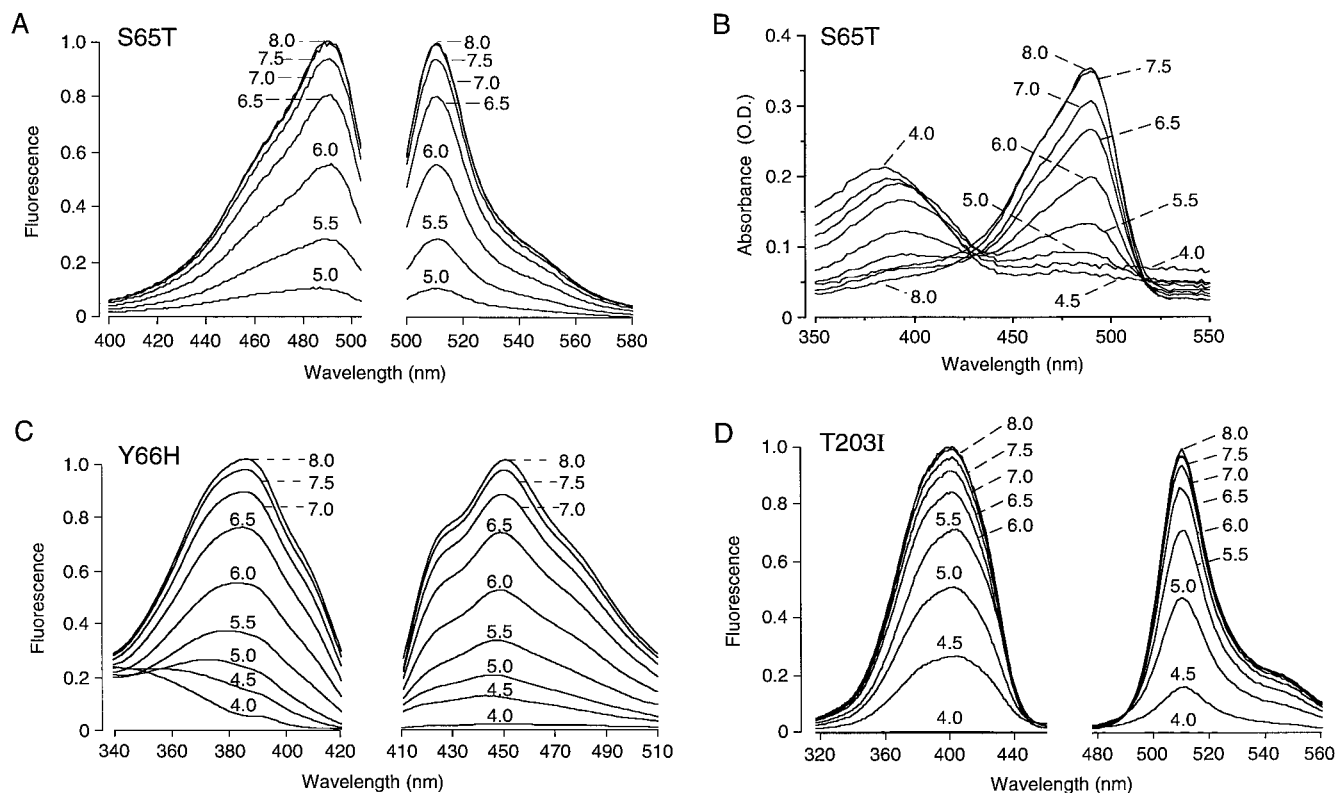


FIGURE 1 pH-dependent spectral properties of GFPs. GFPs were expressed in bacteria and purified as described in Materials and Methods. (A) Fluorescence excitation and emission spectra of GFP-S65T ($\sim 20 \mu\text{g/ml}$) in buffer A at indicated pH. (B) Absorbance spectra of GFP-S65T (0.25 mg/ml). (C and D) Fluorescence spectra of GFP-Y66H and GFP-T203I as in A.

ima were seen. An absorbance at 490 nm, which corresponded to the fluorescence excitation maximum, decreased with pH in parallel to the fluorescence excitation. A second absorbance maximum at ~ 390 nm increased with pH but did not excite GFP-S65T fluorescence at >510 nm. Additional spectral analysis (excitation at 370 nm, emission at 420–470 nm) indicated a very small fluorescence maximum at 450 nm (not shown).

Titration curves were done using other purified GFP mutant proteins to determine whether the pH-dependent spectral properties could be modified by mutagenesis. Fig. 1 C shows that the fluorescence of GFP-Y66H, in which histidine replaces tyrosine in the triamino acid chromophore, was blue-shifted as reported previously (Heim et al., 1994). The spectral intensity decreased with lowered pH, with 50% of maximal intensity at pH ~ 6.0 . In contrast, 50% of maximal intensity was found at pH ~ 5 for GFP-T203I (Fig. 1 D). Absorbance spectra for Y66H and T203I showed single maxima near their corresponding fluorescence excitation maxima, with parallel pH-dependent changes in absorbance and fluorescence (not shown).

The pH titration data for GFP-S65T are summarized in Fig. 2 A. The pH-dependent changes in fluorescence intensity closely paralleled absorbance changes, indicating that it is the GFP-S65T molar absorbance rather than quantum yield (also see fluorescence lifetime data below) that

changes with pH. The titration data were fitted to the following equation:

$$F = A + B/[1 + 10^{n_H(\text{pK}_a - \text{pH})}] \quad (1)$$

with parameters pK_a (pH at 50% maximum) and Hill coefficient n_H (proportional to slope of fluorescence versus pH at pK_a). Parameters A and B are related to signal baseline and gain. Fitted pK_a and n_H were 5.91 and 0.92, respectively. A titration of fluorescein (dashed curve) is shown for comparison. The similar shape of the titration curve for GFP-S65T suggests the involvement of a single amino acid residue in its pH-sensitive mechanism. Fluorescence intensity titrations of Y66H and T203I are shown in Fig. 2 B, along with a titration of F64L/S65T, the GFP-S65T variant with humanized codon usage that also contains an F64L mutation. Fluorescence spectra (not shown) and the pH titration data for GFP-S65T and GFP-F64L/S65T were essentially indistinguishable. Fitted pK_a and n_H values were 5.98 and 0.97 (GFP-F64L/S65T), 5.98 and 0.65 (GFP-Y66H), and 5.05 and 0.91 (GFP-T203I). The Hill coefficient of under unity for Y66H indicates negative cooperativity, suggesting involvement of more than one residue in its pH-sensitive mechanism. These results indicate that mutagenesis can significantly alter GFP pH dependence.

Additional spectroscopic and kinetic studies were done to investigate the mechanism of the GFP pH sensitivity. Fre-

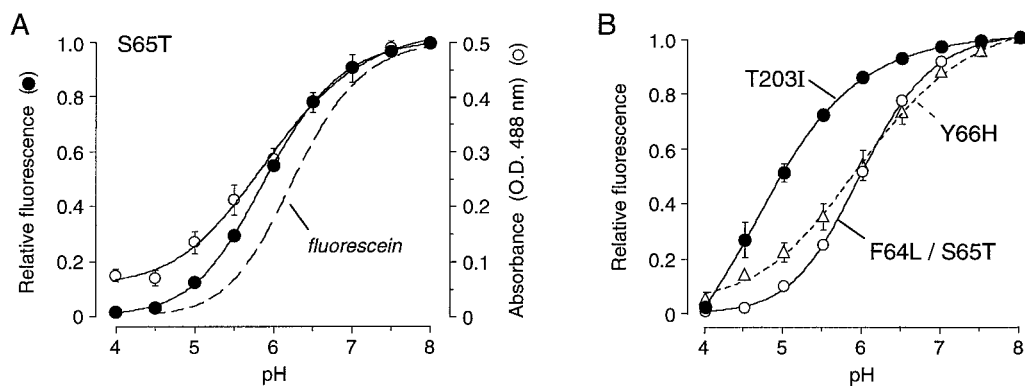


FIGURE 2 pH titrations of GFPs. (A) Fluorescence and absorbance of GFP-S65T as a function of pH. Data were fitted to Eq. 1 with pK_a and n_H parameters given in the text. For comparison, fluorescence titration for fluorescein is shown (- -). (B) Fluorescence of GFP-F64L/S65T, GFP-Y66H, and GFP-T203I as a function of pH with curve fits as in A.

quency-domain fluorimetry showed that GFP-S65T has a single fluorescence lifetime of ~ 2.8 ns that is independent of pH over a wide range of pH values (Fig. 3 A). This result supports the conclusion that pH affects GFP molar absorbance rather than quantum yield. Circular dichroism spectra for GFP-S65T at pH 7.0 and 5.0 did not differ significantly (Fig. 3 B). Acrylamide did not quench GFP-S65T fluorescence (Stern-Volmer constant $< 2 \text{ M}^{-1}$) at pH 5–7 (not shown). Together these results indicate that major changes in secondary structure content do not occur over a pH range in which fluorescence intensity changes by a factor of ~ 15 .

The reversibility of GFP-S65T fluorescence with pH was studied by titrating pH between 6.5 and different pH values (Fig. 3 C). After correcting for dilution, GFP-S65T fluorescence was found to change nearly reversibly between pH 6.5 and pH values down to ~ 5.0 . Fluorescence was not completely reversed at lower pH (< 5), possibly because of a conformational change in the GFP protein and/or decreased solubility. Stopped-flow kinetic measurements were done to distinguish between simple protonation reactions, which would occur in < 1 ms, and protein conformation changes or denaturation, which could occur over millise-

cond and longer times. Nearly all GFP-S65T fluorescence changed in < 1 ms in response to a change in solution pH from 6 to 7 and 7 to 6 (Fig. 3 D). An additional slower process ($t_{1/2}$ of ~ 1 s) was seen for a change in pH from 5 to 3. Together, these results suggest that for pH > 5 , simple protonation of residue(s) on GFP-S65T produces a decrease in molar absorbance at 480 nm and a consequent decrease in fluorescence.

To evaluate the suitability of GFP as a pH indicator in living cells, fluorescence measurements were carried out in cells expressing GFP-F64L/S65T in cytoplasm and various intracellular compartments. Cells were transfected with cDNAs encoding GFP-F64L/S65T alone (for cytoplasmic staining) or in fusion with appropriate organelle targeting sequences as described in Materials and Methods. The fluorescence micrographs in Fig. 4 show bright and specific staining of the targeted cellular compartments. Subsequent measurements of fluorescence were made by microscopy using a photomultiplier to integrate total fluorescence from groups of 10–20 cells.

Intracellular titrations of GFP-F64L/S65T fluorescence versus pH were done using ionophores to equalize intracel-

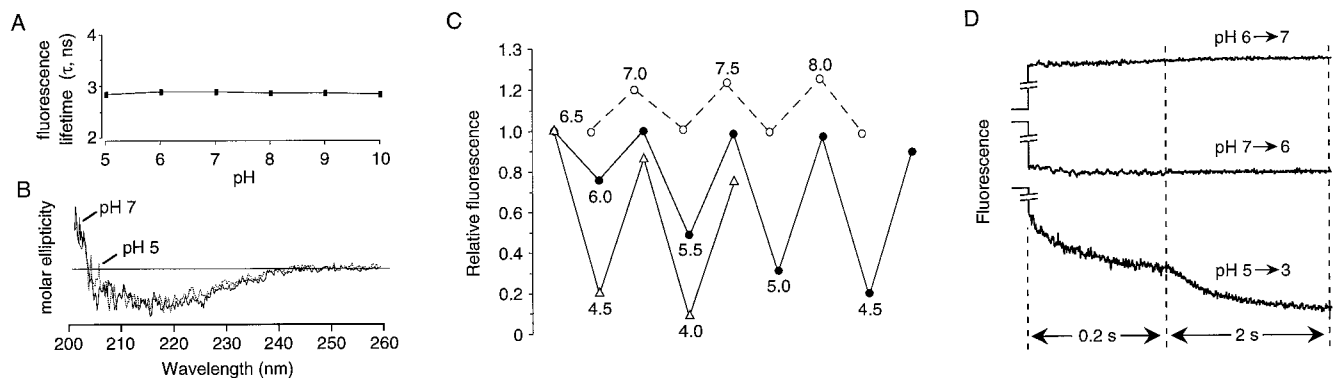


FIGURE 3 pH-dependent properties of GFP-S65T. (A) Fluorescence lifetimes of GFP-S65T ($\sim 50 \mu\text{g/ml}$ in buffer A) measured by phase-modulation fluorimetry. (B) Circular dichroism spectra of solutions from A. (C) Reversibility of GFP-S65T fluorescence with pH changes. Fluorescence was measured in a stirred cuvette. Where indicated, pH changes were established by addition of microliter aliquots of 1 M HCl or NaOH. (D) Stopped-flow kinetic measurement of time course of GFP-S65T fluorescence in response to indicated changes in pH. All measurements were done at 23°C .

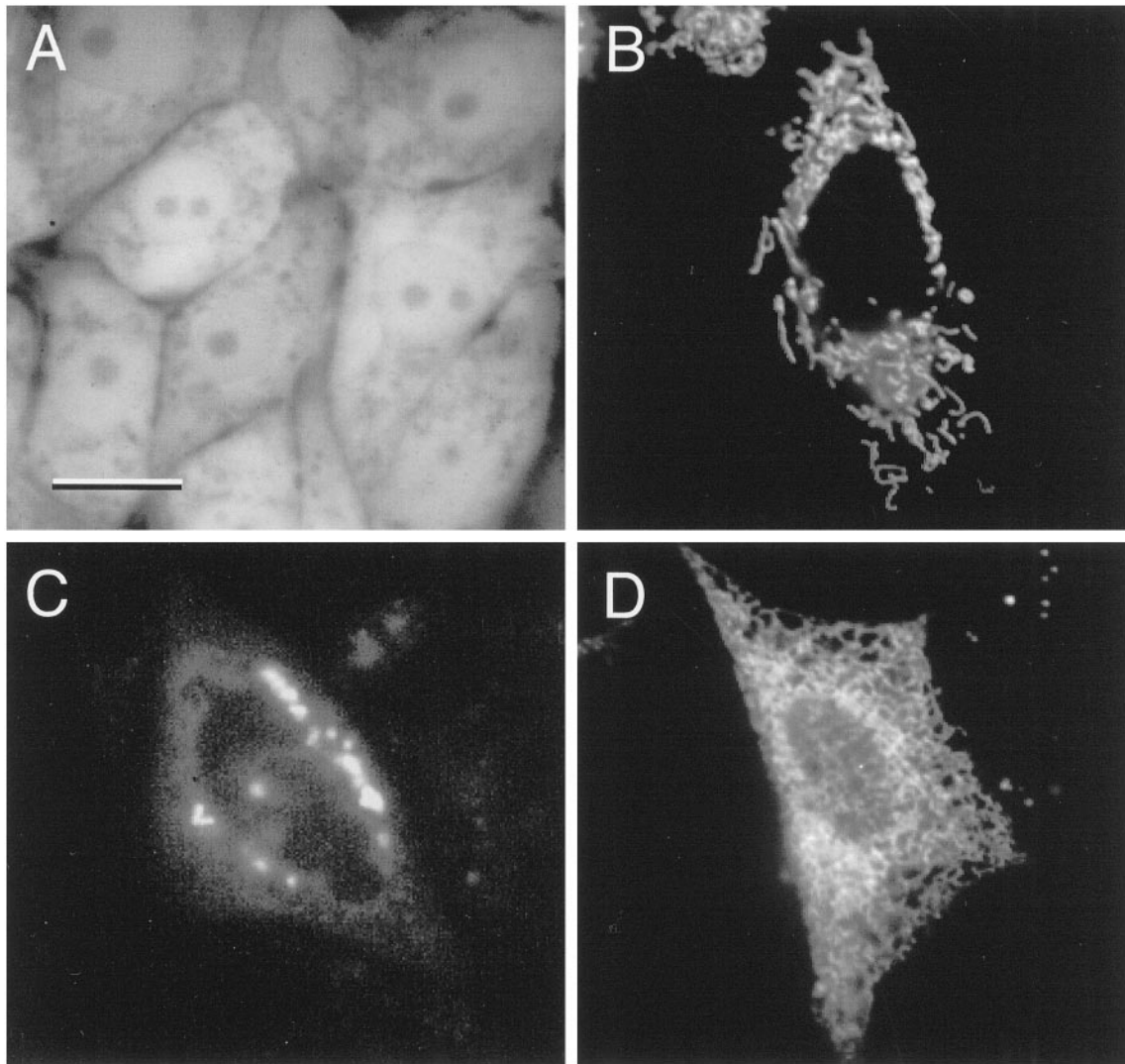


FIGURE 4 Fluorescence micrographs of GFP-F64L/S65T in the cytoplasm of LLC-PK1 cells (A) and the mitochondria (B), Golgi (C), and endoplasmic reticulum (D) of CHO cells. Cells were transfected with GFP-F64L/S65T in fusion with appropriate targeting sequences as described in Materials and Methods.

lular and extracellular pH. Coverglasses containing cells were mounted in a laminar-flow chamber in which perfusion solutions could be exchanged in <1 s. Fig. 5 A (left) shows a representative titration (for GFP-F64L/S65T in cytoplasm) of fluorescence in response to extracellular perfusion with solutions of indicated pH containing ionophores. Large and reversible (not shown) pH-dependent changes in fluorescence were observed. There was little photobleaching and no evidence of photodynamic injury over >1 h using low illumination. Fig. 5 A (right) summarizes averaged pH titration data for four cell preparations. The titration was nearly identical to that for purified GFP-F64L/S65T in saline. A nearly identical titration was obtained using digitonin in place of the ionophores (not shown). Averaged cytoplasmic pH, determined from the fluorescence during perfusion with PBS (not containing ionophores), was 7.35 ± 0.03 .

The response kinetics of cytoplasmic GFP-F64L/S65T fluorescence was measured by addition and removal of NH_4Cl , which promptly alkalinizes (upon addition) and acidifies (upon removal) intracellular compartments because of rapid NH_3 transport and $\text{NH}_3/\text{NH}_4^+$ equilibration. Fig. 5 B shows that NH_4Cl addition (under isosmolar conditions) produces a rapid rise in fluorescence due to intracellular alkalinization, followed by a slower decrease in fluorescence resulting from NH_4 transport and pH regulation. Subsequent replacement of NH_4Cl by NaCl produced a prompt intracellular acidification followed by a slower regulatory phase. The greater magnitude of the fluorescence decrease is due to the nonlinear dependence of GFP-F64L/S65T fluorescence on pH (Fig. 5 A). Therefore, intracellular GFP fluorescence responds rapidly to pH changes.

Experiments were done to demonstrate the usefulness of GFP as an indicator of intraorganellar pH changes. Fig. 5 C

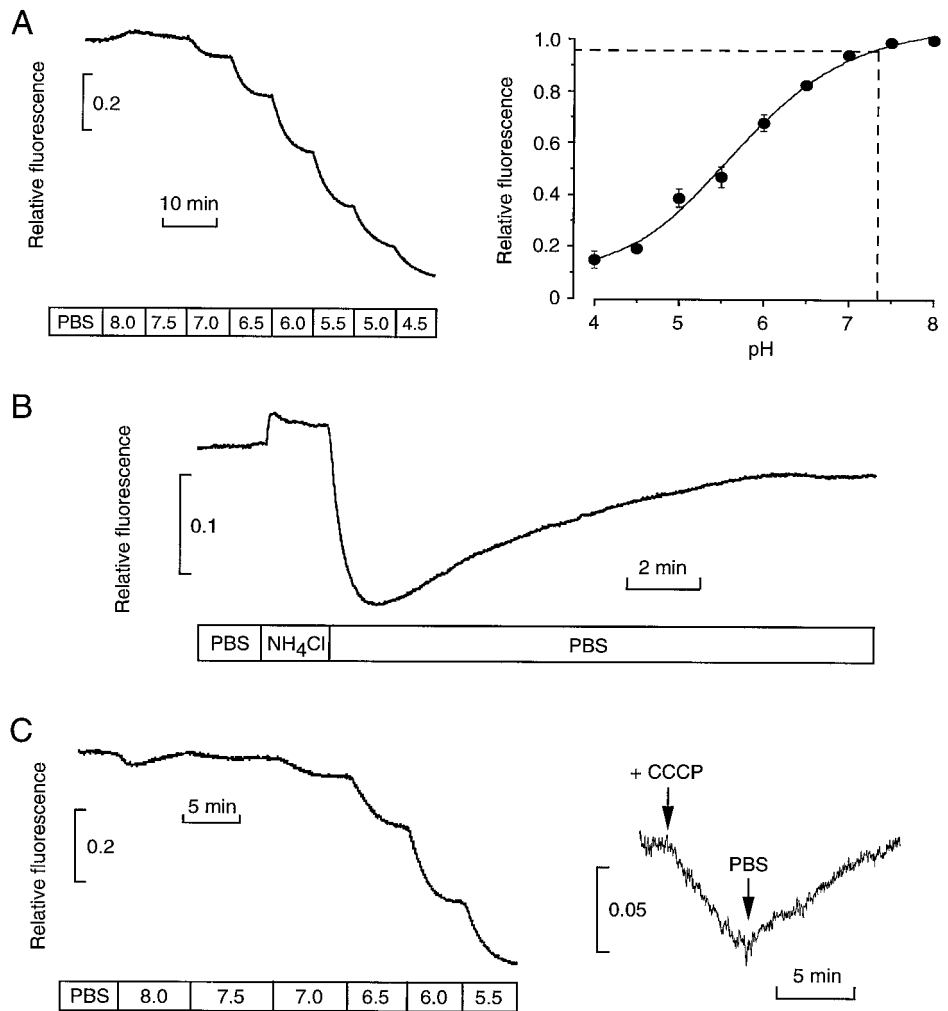


FIGURE 5 GFP as an intracellular pH indicator. (A) Titration of fluorescence versus pH in LLC-PK1 cells expressing GFP-F64L/S65T. Cells were initially perfused with PBS and then with buffer B containing ionophores at indicated pH (see Materials and Methods); (left) Representative titration curve; (right) Averaged fluorescence (SE, $n = 4$) with fit to Eq. 1. (B) Time course of cytoplasmic GFP-F64L/S65T fluorescence in response to replacement of 30 mM NaCl by NH₄Cl and subsequent return to NaCl. (C, left) Titration as in A for CHO cells expressing GFP-F64L/S65T in mitochondria; (right) Response of mitochondrial GFP-F64L/S65T fluorescence to addition of the protonophore CCCP (10 μ M) to the PBS perfusate.

(left) shows a titration of fluorescence versus pH for GFP-F64L/S65T in the mitochondrial matrix. The pH-dependent fluorescence was similar to that for GFP-F64L/S65T in cytoplasm. Mitochondrial pH was relatively high (>7.5) but could not be determined accurately because of the much lower pK_a of GFP-F64L/S65T. A transient decrease in signal was observed upon switching from PBS to the pH 8.0 calibration solution containing ionophores. This decrease is probably due to an increase in proton conductance of the mitochondrial membranes, resulting in proton influx driven by the strong interior negative mitochondrial membrane potential. Fig. 5 C (right) shows that addition of the protonophore CCCP (without other components of the calibration solution) produced reversible acidification of the mitochondrial lumen.

Fig. 6 A shows a pH titration for CHO cells expressing GFP-F64L/S65T in the Golgi compartment. The precise localization of GFP-F64L/S65T (cis- versus medial versus trans-Golgi) was not determined in this study. Addition of the vacuolar proton pump inhibitor bafilomycin A1 produced a slow alkalization, consistent with results obtained when the trans-Golgi lumen was labeled by liposome fusion with a fluorescein-based pH indicator (Seksek et al., 1995)

and by retrograde transport of a fluorescein-labeled verotoxin receptor (Kim et al., 1996). Subsequent perfusion with calibration solutions showed a reversible change in fluorescence similar to results in cytoplasm and mitochondria. Fig. 6 B shows the kinetics of Golgi GFP-F64L/S65T fluorescence in response to addition and removal of the weak acid acetate and the weak base NH₄Cl. Acetate addition produced a prompt acidification (because of rapid acetic acid influx and dissociation) and slower alkalization. Subsequent acetate removal gave a prompt alkalization. NH₄Cl addition and removal produced alkalization and acidification, respectively, as seen for GFP-F64L/S65T in cytoplasm in Fig. 5 B.

DISCUSSION

Unique advantages of GFP as a targeted pH indicator are the ability to measure pH at specific intracellular sites with little background signal and no indicator leakage, and without the toxicities associated with chemical indicators and invasive loading procedures. An ideal fluorescent pH sensor should have high pH sensitivity and specificity, rapid signal re-

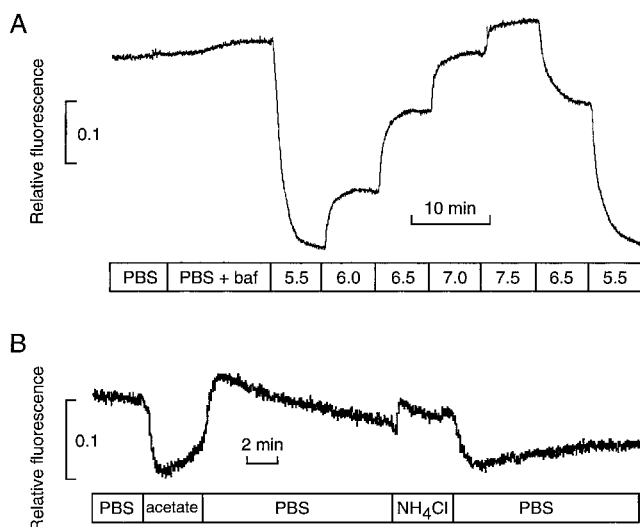


FIGURE 6 Measurement of Golgi changes pH by GFP-F64L/S65T fluorescence. (A) Titration of fluorescence versus pH in CHO cells expressing GFP-F64L/S65T in Golgi. Cells were initially perfused with PBS and then with PBS containing 10 nM bafilomycin A1, followed by calibration solutions (buffer B) containing ionophores at indicated pH. (B) Kinetics of GFP-F64L/S65T fluorescence in response to replacement of 30 mM NaCl in PBS with 30 mM sodium acetate and NH_4Cl .

response to pH changes, and good optical properties. The results here indicate that GFP fulfills many of these requirements. GFP fluorescence changes by $\sim 50\%$ for a 1 pH unit change around its apparent pK_a , similar to the sensitivity of fluorescein-based and other chemical pH indicators. Although the pK_a values of the GFP mutants analyzed here were in the range 5–6, it is likely that the pH sensitivity can be modified by further mutagenesis. Because of the protected environment of the GFP chromophore, its fluorescence should be highly selective for pH; GFP fluorescence and other optical properties are insensitive to quenchers and other chemical agents that strongly influence the optical properties of many chemical chromophores (Swaminathan et al., 1997). GFP fluorescence responds very rapidly to pH changes. The available GFP mutants are brightly fluorescent and have excitation and emission maxima at visible wavelengths, where autofluorescence and photodynamic injury are minimal. Although the pH insensitivity of spectral shape precludes ratio imaging of existing GFPs, it should be possible to couple GFPs with different emission wavelengths and pK_a values to generate a pH indicator suitable for ratio imaging. For cell studies, GFP is an ideal indicator because it is nontoxic, chemically inert, and targetable to selected intracellular locations without leakage or migration.

The pH sensitivity of GFP has implications for its use as a sensor for parameters other than pH. Fluorescence energy transfer between GFP mutants has recently been used in the design of protein sensors to measure protease activity (Heim and Tsien, 1996) and calcium concentration (Romoser et al., 1997; Miyawaki et al., 1997). Because of the pH sensitivity of GFP fluorescence and absorbance, the Forster distance and thus the sensor response will also depend on pH.

Apparent calcium concentrations would thus be different in acidic cellular compartments. GFP mutants with pK_a values much lower than the pH of the sensor environment are needed to eliminate pH effects.

Several experiments suggested that the pH sensitivity of GFP fluorescence at $\text{pH} > 5$ results from protonation-deprotonation of residues at or near the chromophore. The response of GFP fluorescence to pH changes occurred in < 1 ms and was reversible. GFP fluorescence lifetime, fluorescence spectral shape, CD spectra, and fluorescence quenching by acrylamide were also insensitive to pH. At $\text{pH} < 5$, GFP fluorescence responded relatively slowly to pH changes, and the response was not completely reversible. It is thus likely that the GFP unfolds at very low pH, limiting its usefulness as a pH sensor in highly acidic environments.

Crystallographic and spectroscopic data suggest that the protonation state of the phenolic group of the chromophore is responsible for the GFP pH sensitivity. The chromophore in denatured, wild-type GFP has pH-dependent spectral characteristics due to the ionization of the tyrosine 66 phenolic group (Ward et al., 1982). The phenolate form of the chromophore has an absorption maximum at 448 nm compared with that of 384 nm for the uncharged phenol. The pK_a for this transition is 8.1. Based on the excited state dynamics of GFP, it was proposed that wild-type GFP can exist in one of two ground states, A and B, which differ in protonation state of the chromophore (Chattoraj et al., 1996). An excited-state proton transfer reaction rapidly converts state A to intermediate state I, which is slowly converted to state B. State A absorbs at 404 nm and emits at 420–470 nm, state I emits at 500 nm, and state B absorbs at 471 nm and emits at 482 nm. Crystallographic studies confirmed the existence of two ground state conformations each with distinct spectral characteristics (Brjec et al., 1997; Palm et al., 1997). In GFP mutants with excitation maxima at ~ 395 nm, the phenol in tyrosine 66 is uncharged (corresponding to state A), whereas it is in the charged phenolate form in mutants with excitation maxima at 473 nm (corresponding to state B).

Our findings suggest that pH shifts the equilibrium between the GFP A and B ground states. At high pH, the phenolate form of tyrosine is favored so that the B state is populated and excitation and emission occur near 471 nm and 500 nm, respectively (Fig. 1 A). At low pH, the phenol form is favored so that state A is populated and absorbance shifts to 390 nm (Fig. 1 B). The absence of fluorescence emission at 500 nm by excitation at 390 nm is due either to quenching of the I state or to the inability of the I state to convert to the B state. The lower pK_a of 6 for the phenol-phenolate transition in folded GFP compared with denatured GFP is probably due to stabilization of the phenolate form by the network of hydrogen bonds in the folded protein.

The nonunity Hill coefficient for the fluorescence response in Y66H suggests that more than one titratable residue influences the relative stability of the two states. The pH sensitivity for this mutant probably occurs by a mech-

anism in which a water molecule replaces the phenolic oxygen of tyrosine 66 (Palm et al., 1997). Additional work is needed to identify other mutations in GFP that alter pK_a by shifting the equilibrium between the charged and uncharged forms.

The analysis of GFP fluorescence in cell cytoplasm indicated that the dependence of GFP fluorescence on pH was similar to that of the purified protein in saline. Ammonium chloride pulse studies indicated that the GFP signal response is very fast and demonstrated the expected recovery phase involving pH regulatory mechanisms (Roos and Boron, 1981). Continuous measurements of cytoplasmic GFP fluorescence could be made with excellent signal-to-noise ratio and little photobleaching. Fluorescence versus pH calibrations for GFP in various organellar compartments confirmed that the sensitivity of GFP fluorescence to pH did not depend on its location in cells. The experiments in Figs. 5 and 6 demonstrated the ability to follow intracellular pH changes in response to various maneuvers.

The use of GFP as an intracellular pH indicator should permit many types of measurements that cannot easily be accomplished using existing chemical pH indicators. The targeting of GFP to the lumen of organelles allows direct measurements of intraorganellar pH and analysis of pH regulatory mechanisms. There is evidence that trans-Golgi pH is regulated by second messengers including cAMP (Seksek et al., 1995), but the mechanistic basis of this regulation is unknown. Little information is available on pH changes in endoplasmic reticulum, medial and cis-Golgi, mitochondria, and other intracellular compartments. There is provocative evidence that intranuclear pH might be higher than cytoplasmic pH (Seksek and Bolard, 1996); however, the measurements involved indirect chemical indicators with uncertainties in indicator calibration and optical properties. It is thought that chloride channels on organellar membranes are needed to shunt charge to permit the generation of an acidic luminal pH. Intracellular ion transporting mechanisms such as chloride conductance can be measured by coupling ion movement to electrogenic proton transport (by use of ionophores, Biwersi et al., 1994). Finally, selective GFP targeting in transgenic mice should permit measurements of cellular pH *in vivo*.

We thank Catherine Chen for cell culture, Cathy Hoang for initial GFP pH titrations, and Dr. R. Swaminathan for measurement of GFP lifetimes. This work was supported by grants DK43840, DK35124, and HL42368 from the National Institutes of Health and a grant from the National Cystic Fibrosis Foundation.

REFERENCES

- Anderson, M. T., I. M. Tjioe, M. C. Lorincz, D. R. Parks, L. A. Herzenberg, G. P. Nolan, and L. A. Herzenberg. 1996. Simultaneous fluorescence-activated cell sorter analysis of two distinct transcriptional elements within a single cell using engineered green fluorescent proteins. *Proc. Natl. Acad. Sci. USA*. 93:8508–8511.
- Biwersi, J., and A. S. Verkman. 1994. Functional CFTR in the endosomal compartment of CFTR-expressing fibroblasts and T84 cells. *Am. J. Physiol.* 266:C149–C156.
- Bokman, S. H., and W. W. Ward. 1981. Renaturation of *Aequorea victoria* green-fluorescent protein. *Biochem. Biophys. Res. Commun.* 101:1372–1380.
- Brejč, K., T. K. Sixma, P. A. Kitts, S. R. Kain, R. Y. Tsien, M. Ormö, and S. J. Remington. 1997. Structural basis for dual excitation and photoisomerization of the *Aequorea victoria* green fluorescent protein. *Proc. Natl. Acad. Sci. USA*. 94:2306–2311.
- Chalfie, M., Y. Tu, G. Euskirchen, W. W. Ward, and D. C. Prasher. 1994. Green fluorescent protein as a marker for gene expression. *Science*. 263:802–805.
- Chattoraj, M., B. A. King, G. U. Bublitz, and S. G. Boxer. 1996. Ultra-fast excited state dynamics in green fluorescent protein: multiple states and proton transfer. *Proc. Natl. Acad. Sci. USA*. 93:8362–8367.
- Cole, N. B., C. L. Smith, N. Sciaky, M. Terasaki, M. Eddin, and J. Lippincott-Schwartz. 1996. Diffusional mobility of Golgi proteins in membranes of living cells. *Science*. 273:797–801.
- Cormack, B. P., R. H. Valdivia, and S. Falkow. 1996. FACS-optimized mutants of the green fluorescent protein (GFP). *Gene*. 173:33–38.
- Cubitt, A. B., Heim, R., S. R. Adams, A. E. Boyd, L. A. Gross, and R. Y. Tsien. 1995. Understanding, improving and using green fluorescent proteins. *Trends Biochem. Sci.* 20:448–455.
- De Giorgi, F., M. Brini, C. Bastianutto, R. Marsault, M. Montero, P. Pizzo, R. Rossi, and R. Rizzuto. 1996. Targeting aequorin and green fluorescent protein to intracellular organelles. *Gene*. 173:113–117.
- Gerdes, H.-H., and C. Kaether. 1996. Green fluorescent protein: applications to cell biology. *FEBS Lett.* 389:44–47.
- Girotti, M., and G. Banting. 1996. TGN38-green fluorescent protein hybrid proteins expressed in stably transfected eukaryotic cells provide a tool for the real-time, *in vivo* study of membrane traffic pathways and suggest a possible role for rat TGN38. *J. Cell. Sci.* 109:2915–2926.
- Hampton, R. Y., A. Koning, R. Wright, and J. Rine. 1996. *In vivo* examination of membrane protein localization and degradation with green fluorescent protein. *Proc. Natl. Acad. Sci. USA*. 93:828–833.
- Heim, R., A. B. Cubitt, and R. Y. Tsien. 1995. Improved green fluorescence. *Nature*. 373:663–664.
- Heim, R., D. C. Prasher, and R. Y. Tsien. 1994. Wavelength mutations and posttranslational autooxidation of green fluorescent protein. *Proc. Natl. Acad. Sci. U.S.A.* 91:12501–12504.
- Heim, R., and R. Y. Tsien. 1996. Engineering green fluorescent protein for improved brightness, longer wavelengths and fluorescence resonance energy transfer. *Curr. Biol.* 6:176–182.
- Kim, J. H., C. A. Lingwood, D. B. Williams, W. Furuya, M. F. Manolson, and S. Grinstein. 1996. Dynamic measurement of the pH of the Golgi complex in living cells using retrograde transport of the verotoxin receptor. *J. Cell Biol.* 134:1387–1399.
- Kimata, Y., M. Iwaki, C. R. Lim, and K. Kohno. 1997. A novel mutation which enhances the fluorescence of green fluorescent protein at high temperatures. *Biochem. Biophys. Res. Commun.* 232:69–73.
- Lim, C. R., Y. Kimata, M. Oka, K. Nomaguchi, and K. Kohno. 1995. Thermosensitivity of green fluorescent protein fluorescence utilized to reveal novel nuclear-like compartments in a mutant nucleoporin NSP1. *J. Biochem.* 118:13–17.
- Liu, J., T. E. Hughes, and W. C. Sessa. 1997. The first 35 amino acids and fatty acylation sites determine the molecular targeting of endothelial nitric oxide synthase into the Golgi region of cells: a green fluorescent protein study. *J. Cell Biol.* 137:1525–1535.
- Masri, K. A., H. E. Appert, and M. N. Fukada. 1988. Identification of the full-length coding sequence for human galactosyltransferase. *Biochem. Biophys. Res. Commun.* 157:657–663.
- Miyawaki, A., J. Lloppis, R. Heim, J. M. McCaffery, J. A. Adams, M. Ikura, and R. Y. Tsien. 1997. Fluorescent indicators for Ca^{2+} based on green fluorescent proteins and calmodulin. *Nature*. 388:882–887.
- Munro, S., and H. R. B. Pelham. 1987. A C-terminal signal prevents secretion of luminal ER proteins. *Cell*. 48:899–907.
- Ormö, M., A. B. Cubitt, K. Kallio, L. A. Gross, R. Y. Tsien, and S. J. Remington. 1996. Crystal structure of the *Aequorea victoria* green fluorescent protein. *Science*. 273:1392–1395.
- Palm, G. J., A. Zdanov, G. A. Gaitanaris, R. Stauber, G. N. Pavlakis, and A. Wlodawer. 1997. The structural basis for spectral variations in green fluorescent protein. *Nature Struct. Biol.* 4:361–365.

- Partikian, A., B. P. Ölveczky, R. Swaminathan, Y. Li, and A. S. Verkman. 1998. Rapid diffusion of green fluorescent protein in the mitochondrial matrix. *J. Cell Biol.* In press.
- Prasher, D. C., V. K. Eckenrode, W. W. Ward, F. G. Prendergast, and M. J. Cormier. 1992. Primary structure of the *Aequorea victoria* green-fluorescent protein. *Gene*. 111:229–233.
- Rizzuto, R., M. Brini, F. De Giorgi, R. Rossi, R. Heim, R. Y. Tsien, and T. Pozzan. 1996. Double labelling of sub-cellular structures with organelle-targeted GFP mutants in vivo. *Curr. Biol.* 6:183–188.
- Rizzuto, R., M. Brini, P. Pizzo, M. Murgia, and T. Pozzan. 1995. Chimeric green fluorescent protein: a new tool for visualizing subcellular organelles in living cells. *Curr. Biol.* 5:635–642.
- Romoser, V. A., P. M. Hinkle, and A. Persechini. 1997. Detection in living cells of Ca^{2+} -dependent changes in the fluorescence emission of an indicator composed of two green fluorescent protein variants linked by a calmodulin-binding sequence. *J. Biol. Chem.* 272:13270–13274.
- Roos, A., and W. F. Boron. 1981. Intracellular pH. *Physiol. Rev.* 61:296–434.
- Sasavage, N. L., J. H. Hilson, S. Horwitz, and F. M. Rottman. 1982. Nucleotide sequence of bovine prolactin messenger RNA: evidence for sequence polymorphism. *J. Biol. Chem.* 257:678–681.
- Seksek, O., J. Biwersi, and A. S. Verkman. 1995. Direct measurement of trans-Golgi pH in living cells and regulation by second messengers. *J. Biol. Chem.* 270:4967–4970.
- Seksek, O., and J. Bolard. 1996. Nuclear pH gradient in mammalian cells revealed by laser scanning microspectrofluorimetry. *J. Cell Sci.* 109:257–262.
- Swaminathan, R., C. P. Hoang, and A. S. Verkman. 1997. Photobleaching recovery and anisotropy decay of green fluorescent protein GFP-S65T in solution and cells: cytoplasmic viscosity probed by green fluorescent protein translational and rotational diffusion. *Biophys. J.* 72:1900–1907.
- Terasaki, M., L. A. Jaffe, G. R. Hunnicutt, and J. A. Hammer. 1996. Structural change of the endoplasmic reticulum during fertilization: evidence for loss of membrane continuity using the green fluorescent protein. *Dev. Biol.* 179:320–328.
- Ward, W. W., C. W. Cody, R. C. Hart, and M. J. Cormier. 1980. Spectrophotometric identity of the energy transfer chromophores in renilla and aequora green-fluorescent proteins. *Photochem. Photobiol.* 31:611–615.
- Ward, W. W., H. J. Prentice, A. F. Roth, C. W. Cody, and S. C. Reeves. 1982. Spectral perturbations of the *Aequorea* green-fluorescent protein. *Photochem. Photobiol.* 35:803–808.
- Yang, F., L. G. Moss, and G. N. Phillips, Jr. 1996. The molecular structure of green fluorescent protein. *Nature Biotech.* 14:1246–1251.
- Zolotukhin, S., M. Potter, W. W. Hauswirth, J. Guy, and N. Muzyczka. 1996. A “humanized” green fluorescent protein cDNA adapted for high-level expression in mammalian cells. *J. Virol.* 70:4646–4654.